IUPAC Technical Report

Clive Bucknall*, Volker Altstädt, Dietmar Auhl, Paul Buckley, Dirk Dijkstra, Andrzej Galeski, Christoph Gögelein, Ulrich A. Handge, Jiasong He, Chen-Yang Liu, Goerg Michler, Ewa Piorkowska, Miroslav Slouf, Iakovos Vittorias and Jun Jie Wu

Structure, processing and performance of ultra-high molecular weight polyethylene (IUPAC Technical Report). Part 4: sporadic fatigue crack propagation

https://doi.org/10.1515/pac-2019-0408
Received April 16, 2019; accepted March 20, 2020

Abstract: Fatigue tests were carried out on compression mouldings supplied by a leading polymer manufacturer. They were made from three batches of ultra-high molecular weight polyethylene (UHMWPE) with weight-average relative molar masses, $\overline{M}_W$, of about 0.6×10^6, 5×10^6 and 9×10^6. In 10 mm thick compact tension specimens, crack propagation was so erratic that it was impossible to follow standard procedure, where crack-tip stress intensity amplitude, ΔK, is raised incrementally, and the resulting crack propagation rate, da/dN, increases, following the Paris equation, where a is crack length and N is number of cycles. Instead, most of the tests were conducted at fixed high values of ΔK. Typically, da/dN then started at a high level, but decreased irregularly during the test. Micrographs of fracture surfaces showed that crack propagation was sporadic in these specimens. In one test, at $\Delta K = 2.3$ MPa $m^{0.5}$, there were crack-arrest marks at intervals Δa of about 2 μm, while the number of cycles between individual growth steps increased from 1 to more than 1000 and the fracture surface showed increasing evidence of plastic deformation. It is concluded that sporadic crack propagation was caused by energy-dissipating crazing, which was initiated close to the crack tip under plane strain conditions in mouldings that were not fully consolidated. By contrast, fatigue crack propagation in 4 mm thick specimens followed the Paris equation approximately. The results from all four reports on this project are reviewed, and the possibility of using fatigue testing as a quality assurance procedure for melt-processed UHMWPE is discussed.

Article note: Sponsoring body: IUPAC Polymer Division: see more details on page 1536.

***Corresponding author: Clive Bucknall,** B 61 School of Aerospace, Transport & Manufacturing, Cranfield University, Bedford, MK43 0AL, UK, e-mail: clivebucknall@aol.com
Volker Altstädt: Department of Polymer Engineering, Universität Bayreuth, Bayreuth, Germany
Dietmar Auhl: Fakultät III – Werkstoffwissenschaft Technische, Universität Berlin, D-10623, Berlin, Germany
Paul Buckley: Department of Engineering Science, University of Oxford, Oxford, OX1 3PJ, UK
Dirk Dijkstra: Covestro Deutschland AG, Leverkusen, Germany
Andrzej Galeski and Ewa Piorkowska: Centre for Molecular and Macromolecular Sciences, Polish Academy of Sciences, Lodz, Poland
Christoph Gögelein: Arlanxeo Deutschland GmbH, Dormagen, Germany
Ulrich A. Handge: Institute of Polymer Research, Helmholtz-Zentrum Geesthacht, Max-Planck-Strasse 1, Geesthacht, 21502, Germany
Jiasong He and Chen-Yang Liu: Chinese Academy of Sciences, Laboratory of Polymer Science and Materials, Beijing, China
Goerg Michler: Martin-Luther-Universität Halle-Wittenberg, Halle-Wittenberg, Germany
Miroslav Slouf: Institute of Macromolecular Chemistry CAS, Prague, Czech Republic
Iakovos Vittorias: Omya International AG, Baslerstrasse 42, CH-4665, Oftringen, Switzerland
Jun Jie Wu: Department of Engineering, Durham University, Stockton Road, Durham, DH1 3LE, UK

Keywords: Consolidation; crazing; fatigue; fusion defects; IUPAC Polymer Division; quality assurance; UHMWPE.

CONTENTS

1 Introduction

This is the fourth and final report from IUPAC Sub-Committee 4.2.1 (Structure and Properties of Commercial Polymers), which formed a Task Group to assess current methods of quality assurance and quality control during the manufacture of ultra-high molecular weight polyethylene[1] (UHMWPE), which were known to be inadequate, and, if possible, to recommend improvements. Commercial grades of UHMWPE, which are used to make prosthetic joint implants, almost always contain 'fusion defects', in which the bonding between the original reactor powder particles is less than perfect. However, there have been no satisfactory methods for detecting and classifying these defects, or for making quantitative assessments of any damaging effects they might have on the performance in prosthetic joint implants. During the course of this study, we have found that fatigue crack propagation tests can produce striking evidence for weak inter-particle bonding in compression-moulded UHMWPE. Consequently, the results obtained from those fatigue tests are presented in this separate report, rather than being included in Part 3 of the series, which covers all other mechanical properties.

2 Experiments and results

2.1 Materials

Three large batches of linear polyethylene powder with weight-average relative molar mass, $\overline{M}_W$, of approximately 0.6×10^6, 5×10^6 and 9×10^6 were prepared exclusively for this project by a leading manufacturer of UHMWPE. The batches are identified by the codenames PE06, PE5 and PE9, respectively. For convenience, the term UHMWPE is applied to all three materials featured in this article, although PE06 should strictly be classified as HMWPE, because its $\overline{M}_W$ is below 10^6. All of the experimental data presented in this report were obtained from tests on compression mouldings that were made by the polymer producer specifically for this project in 2009 and 2010. It should be noted that none of the samples supplied contained any additives, at the request of Task Group members, and they should not be regarded as standard, commercially available, products. Many commercial grades of UHMWPE are known to contain additives, such as Vitamin E.

The specialized equipment used to study fatigue crack propagation in Bayreuth was not made available until 2015. Because the polymer manufacturer was unable to supply fresh mouldings at that time, all of the fatigue data

1 The term 'molecular weight', which has a long history, is often used as a synonym for 'relative molecular mass'.

presented in this report were therefore obtained from surplus mouldings held in storage by other members of the IUPAC Task Group. In other words, the mouldings were all at least five years old when they were tested. The possible effects of a long period in storage should be taken into account in any discussion of their unusual mechanical properties; prosthetic implants are of course required to operate for much longer than 5 years, under very demanding conditions, at 37 °C. Most of the fatigue tests were carried out on 10 mm thick specimens, but some measurements were also made on 4 mm thick specimens towards the end of the project.

2.2 Fatigue crack propagation test results

An extensive program of testing was carried out at Bayreuth University using an Instron® servo-hydraulic testing machine fitted with specialized software that calculates crack opening displacement from strain gauge measurements on rectangular compact tensile specimens. In conjunction with data on applied force F, these measurements are used both to calculate current crack length, a, and to adjust the applied force amplitude, ΔF, to the levels required to obtain selected values of ΔK. No visual measurements of crack growth were made during the tests carried out during the present investigation. The same equipment and procedure was previously used to study fatigue in a range of materials, and these studies showed that the method is reliable and effective for well-consolidated polymers, giving results that are consistent with those obtained using visual observations to monitor fatigue crack propagation [1–7].

The test specimens were 39.6 mm high and 36.5 mm wide, measured from the axes of the loading pins. Forces were applied through 6.6 mm diameter pins. The saw-cut starter cracks were sharpened cryogenically and temperature distributions across the specimens were recorded using an infra-red camera. An MTS strain gauge was clamped to the narrow front face of the specimen using rubber bands. Tests were carried out in a temperature-controlled room at 23 °C and 50 % relative humidity, with the stress amplitude ratio $R = K_{min}/K_{max} = 0.1$. Initially the test frequency was 10 Hz, but this was later lowered to 3 Hz in order to minimize viscoelastic heating at the crack tip. Most of the test specimens were 10 mm thick, but some tests were carried out on 4 mm thick specimens during the later stages of the investigation.

The original plan was to follow standard fatigue testing procedure, in which ΔK is raised incrementally and the resulting increases in da/dN are recorded. However, it proved impossible to apply this procedure to any of the 10 mm thick specimens. There were two basic problems: (a) it was extremely difficult to initiate crack propagation at low ΔK and (b) when the software eventually registered some crack growth, raising ΔK did not necessarily result in an increase in the recorded crack growth rate.

These difficulties are illustrated in Figs. 1 and 2, which display data from a single fatigue test on PE06 in two different ways. There was no detectable crack growth at ΔK levels below 1.4 MPa m$^{0.5}$, and when propagation began it was spasmodic. This stage was followed by a period in which ΔK was raised incrementally from

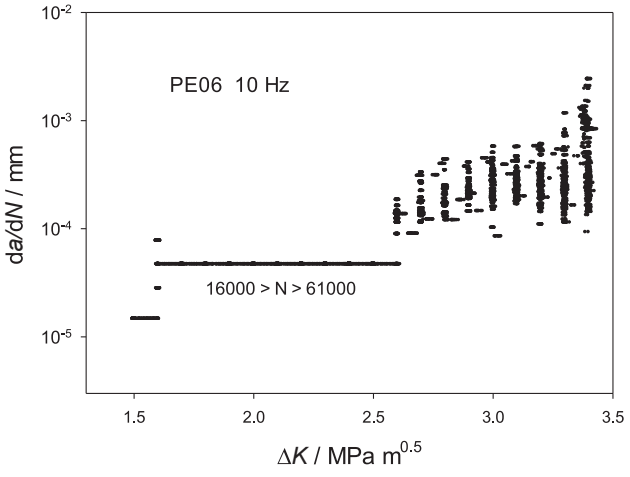

Fig. 1: Fatigue crack growth in a 10 mm thick PE06 CT specimen, plotted against crack-tip stress intensity amplitude ΔK, showing erratic variations in da/dN.

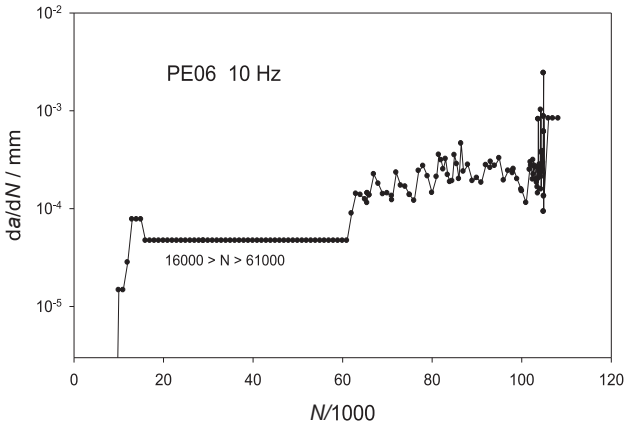

Fig. 2: Fatigue crack growth rate data from Fig. 1, replotted against the number of load cycles.

1.6 to 2.5 MPa $m^{0.5}$ in steps of 0.1 MPa $m^{0.5}$, with ΔK held constant for about 4500 cycles after each step. During this period, the recorded crack growth rate, da/dN, remained precisely constant at 46.820 nm per cycle, which lasted for more than 45 000 cycles. Such an improbable degree of reproducibility, combined with other relevant observations, which will be described later, strongly suggest that no true crack growth took place over this period and that the continual increases in specimen compliance recorded by the software were due, at least in part, to the formation of an expanding craze zone around a static crack tip.

Discontinuous fatigue crack growth in UHMWPE was first reported by Zeng *et al.* [3], who carried out tests on 10 mm thick compact tension specimens. The polymer was crosslinked using high-energy radiation and tested at 1 Hz in saline solution at 37 °C. When testing began at $\Delta K \geq 2.0$ MPa $m^{0.5}$, da/dN followed the Paris Law, as expected, with striations on the surface corresponding to the measured crack growth rate da/dN. Those results confirm that crack growth was essentially brittle at high stress-intensity levels, with only a small amount of plasticity at the crack tips. By contrast, when the initial level of ΔK was reduced to 1.8 MPa $m^{0.5}$ and raised incrementally to 2.0 MPa $m^{0.5}$, crack growth was discontinuous, with da/dN varying randomly between zero and 10 nm per cycle and specimens showing strong evidence of ductile failure. Optical microscopy applied to these specimens revealed extensive blunting of the original sharpened pre-cracks and the formation of crazed damage zones combined with some plastic deformation, which brought crack growth to a halt. This initial stage in the fracture process was eventually followed by re-initiation of crack growth, which continued for 0.5 mm before being arrested for a second time. The crack tip then remained static for up to a million cycles before the same pattern of crack growth and arrest was repeated. Zeng *et al.* concluded that the erratic behaviour was caused by crazing from the crack tip combined with shear band formation on planes at ±45 ° to the crack plane. These deviations from standard crack growth behaviour are consistent with failure under

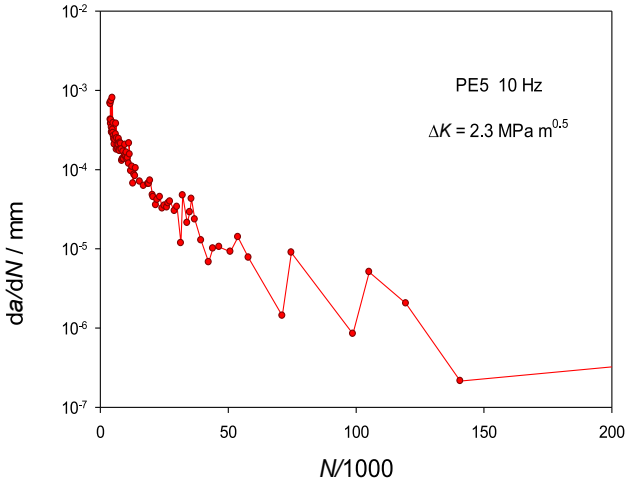

Fig. 3: Fatigue crack growth rates for a 10 mm thick PE5 specimen cycled at 10 Hz, with ΔK nominally held constant at 2.3 MPa $m^{0.5}$.

plane strain conditions at low ΔK, but are modest in comparison with those illustrated in Figs. 1–3, 6 and 7. The results obtained by Zeng *et al.* indicate that cyclic loading under plane strain conditions caused small-scale, distributed, cohesive failure around the crack tip, thereby enabling the polymer to yield.

After the remarkable period of apparent stability recorded in Fig. 1, the next stage of crack growth also had unusual features, which are shown more clearly in Fig. 2, where the same values of da/dN are plotted against the number of loading-unloading cycles N. This diagram shows that the increase in ΔK from 2.5 to 2.6 MPa $m^{0.5}$ had no immediate effect on the recorded propagation rate, which remained unchanged for the first 300 cycles at the higher ΔK level. Crack growth then became unstable; da/dN began to jump unpredictably at irregular intervals, running for up to 300 cycles at a constant growth rate before moving to a different level. This happened six times at ΔK = 2.6 MPa $m^{0.5}$. Most of the shifts were in the upward direction, but da/dN also decreased for a short period.

When ΔK was eventually raised to 2.7 MPa $m^{0.5}$, a similar pattern developed, beginning with a step increase in da/dN, which then rose and fell erratically. Towards the end of the test, where ΔK was 3.4 MPa $m^{0.5}$, the ratio of the highest to the lowest recorded rates of propagation was approximately 30. Finally, after about 105 000 cycles, when the crack length a reached 25 mm, crack growth ended in plastic collapse on the remaining ligament, which at that stage was 8 mm long. Dimples were clearly visible at the edges of the crack, showing that the specimen ultimately failed in plane stress.

Erratic fatigue crack propagation behaviour, similar to that illustrated in Figs. 1 and 2, was also exhibited in tests on both PE5 and PE9. There was little to be learned from these tests, and most of them were therefore terminated before they reached final fracture. Following numerous unsuccessful attempts to produce conventional fatigue crack growth patterns in any of the three UHMWPE materials supplied for this project, a new approach was adopted. The aims in this second stage of the investigation were to identify conditions under which da/dN showed some stability and then to investigate the factors responsible for that stability. Testing was restricted to PE5 specimens and measurements were made with ΔK held constant at selected high levels, which would normally result in crack propagation at constant speeds.

Data from one test conducted in this way, with ΔK held constant at 2.3 MPa $m^{0.5}$, are presented in Fig. 3. Initially, recorded values of da/dN were close to 1 μm/cycle, but the propagation rate subsequently fell fairly rapidly, eventually reaching a much lower level. The scanning electron micrographs presented in Fig. 4, which were obtained from the same specimen, throw some light on this strange behaviour. At the beginning of the test, crack-arrest lines running roughly parallel to the original crack tip were about 2 μm apart. To a first approximation, this observation is consistent with the crack growth rate data recorded by the software at the beginning of the test. However, the calculated values of da/dN subsequently fell from 1 μm per cycle to less than 1 nm per cycle, while the spacing between crack-arrest lines remained approximately constant at about 2 μm and the effects of plastic deformation became increasingly apparent on the fracture surface. From this evidence, it is clear that the intervals between crack growth steps increased enormously and somewhat irregularly throughout the course of this test, while the lengths of those growth steps appear to have remained essentially constant at about 2 μm per cycle. In other words, true crack propagation became increasingly sporadic during the test, presumably because a fluctuating damage zone formed (and occasionally failed) around the propagating crack tip. The full implications of this experimental evidence are considered in more detail in the Discussion.

In the third stage of the investigation, the imposed frequency was reduced to 3 Hz in order to minimize viscoelastic heating. Under these conditions, it was possible to produce 'normal', stable fatigue crack growth in one specimen, as illustrated in Fig. 5, where (after 3373 loading-unloading cycles with no detectable propagation) da/dN increased slowly, from about 2 μm/cycle to about 3 μm/cycle, over about 4000 cycles.

At lower stress amplitudes (ΔK between 1.5 and 2.2 MPa $m^{0.5}$), crack growth patterns in PE5 were invariably erratic. Figs. 6 and 7 show results from a single test, in which ΔK was initially held at 2.0 MPa $m^{0.5}$ for 800 000 cycles, then raised to 2.1 MPa $m^{0.5}$. At the lower ΔK, da/dN decreased erratically, by a factor of 1000, over 800 000 cycles. Raising ΔK by 5 % caused da/dN to rise abruptly, by a factor of 100, before falling sharply. With increasing crack length, da/dN rose and fell several times before plastic collapse brought the test to a halt

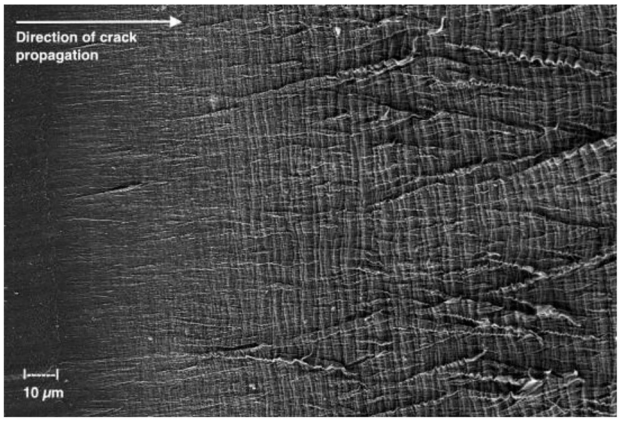

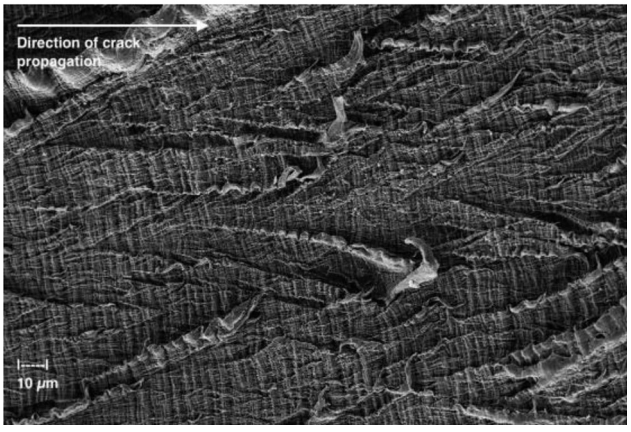

Fig. 4: Fracture surface of 10 mm thick PE5 compact tension specimen subjected to fatigue test at 10 Hz with $\Delta K = 2.3$ MPa m$^{0.5}$. Top: near the notch tip. Bottom: in the end region. Crack propagation from left to right – see arrow. Note 10 μm scale bar at bottom left of micrographs.

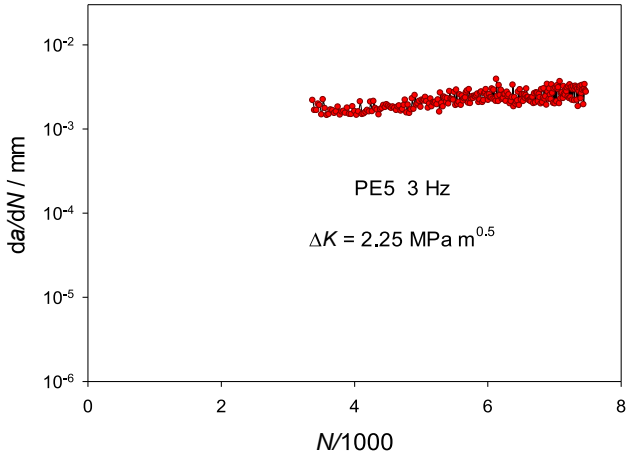

Fig. 5: Delayed stable fatigue crack growth in 10 mm thick PE5 specimen at 3 Hz, with $\Delta K = 2.25$ MPa m$^{0.5}$.

at $a = 17$ mm. Similar erratic behaviour had been observed previously in fatigue tests at 10 Hz on PE9. In all three grades of UHMWPE, yielding on the net section occurred after about 1.1 million cycles.

By contrast, a 10 mm thick PE06 compact tension specimen exhibited very high toughness under continuously increasing loading at –40 °C, as illustrated in Fig. 8. In this test, as the applied force increased, initial steady crack growth was followed by yielding on the net section. The specimen showed no evidence of irregularities in crack propagation behaviour. It appears that the erratic crack propagation behaviour exhibited

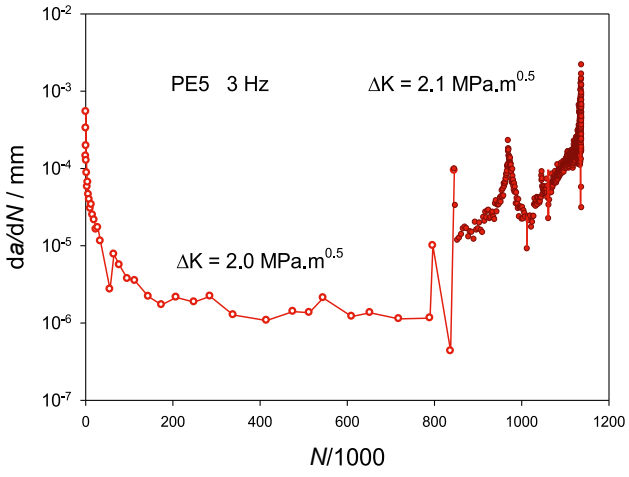

Fig. 6: Unstable fatigue crack growth at 3 Hz in a 10 mm thick PE5 specimen, with Δ*K* raised from 2.0 (circles) to 2.1 MPa $m^{0.5}$ (solid points).

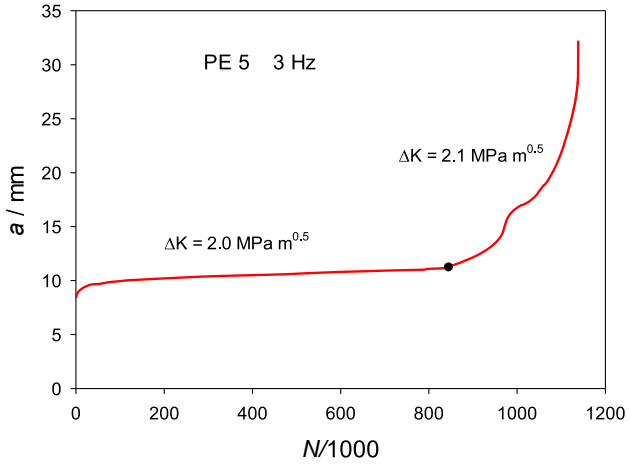

Fig. 7: Data from fatigue test illustrated in Fig. 6, replotted to show relationship between crack length *a* and number of cycles *N*.

Fig. 8: A 10 mm thick PE06 compact tension specimen tested at −40 °C, showing a high level of ductility under steadily increasing grip separation.

by all of the 10 mm UHMWPE mouldings prepared for this project was restricted to fatigue specimens that had initially been subjected to load cycling at low or medium Δ*K* levels. In light of these observations, no monotonic compact tension tests were carried out on PE5 or PE9.

A possible explanation for the complex fatigue behaviour illustrated in Figs. 1–3, 6 and 7 is that all three grades of UHWMPE are susceptible to internal damage close to the crack tip when tests are carried out under

plane strain conditions. With this in mind, an additional program of fatigue testing at 3 Hz was initiated, with the thickness of the compact tension specimens reduced to 4 mm. Results from tests on these thinner samples are presented in Fig. 9–11. They show some scatter at $\Delta K < 2.25$ MPa m$^{0.5}$, possibly because localized plane strain

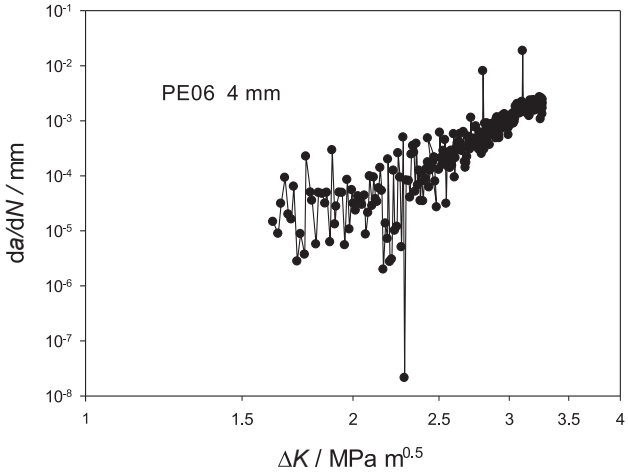

Fig. 9: Fatigue crack growth data from a test at 3 Hz on a 4 mm thick PE06 specimen.

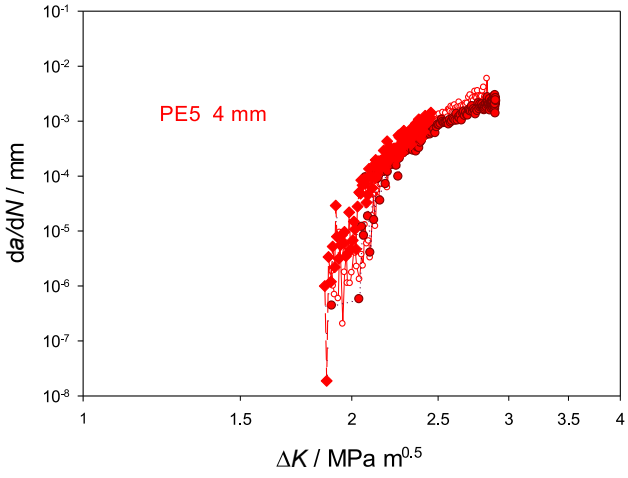

Fig. 10: Fatigue crack growth data from tests at 3 Hz on three 4 mm thick PE5 specimens, represented by diamonds, open circles, and closed circles with dark borders.

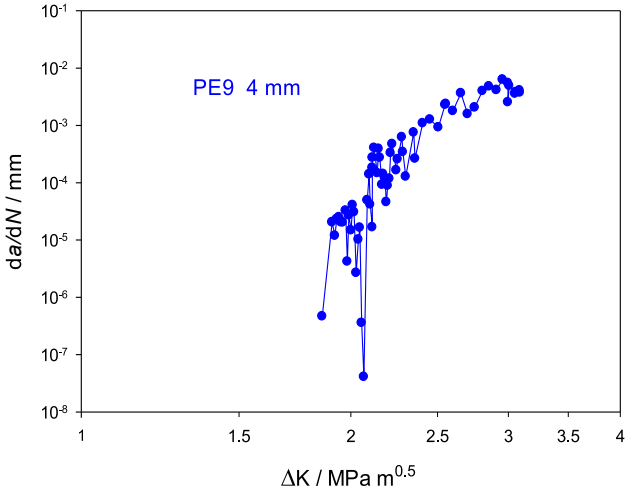

Fig. 11: Fatigue crack growth data from a test at 3 Hz on a 4 mm thick PE9 specimen.

conditions near the central planes of the specimens still had a marginal effect on crack propagation during the early stages of each test. Nevertheless, the difference in fatigue behaviour between 4 and 10 mm thick specimens is striking. It supports the conclusions that bonding between powder particles[2] in the compression mouldings supplied for this project by the polymer manufacturer was less than perfect, and that distributed crazing strongly affected crack growth in fatigue tests under plane strain conditions, where crack tip stresses are strongly triaxial. This hypothesis is examined in more detail in the Section 3.

3 Discussion

Standard fatigue testing starts at a low value of ΔK, which is increased gradually until crack growth is detected. After an initial transitional period, propagation almost invariably follows the Paris equation:

$$\frac{da}{dN} = C(\Delta K)^m \tag{1}$$

where C and m are constants with magnitudes determined by the properties of the test material. The literature contains many examples of conventional fatigue crack growth in UHMWPE, in accordance with Equation (1) [1–7]. Most notably, Gencur *et al.* [5] studied fatigue crack propagation in 10 and 20 mm thick ram-extruded UHMWPE specimens, which were either freshly-prepared or crosslinked by irradiation. In both sets of samples, the data fitted Equation (1) perfectly. The contrast in fatigue behaviour between those ram-extruded specimens and the compression-moulded specimens featured in Figs. 1–3, 6 and 7 is striking. It demonstrates that melt-processing conditions can have a profound effect on the strength of consolidation in UHMWPE. In the present study, numerous attempts were made to carry out fatigue tests on 10 mm thick specimens in the usual way, but they had to be abandoned because it was so difficult to initiate continuous crack growth in any of the samples.

In the present study, the results from tests on 4 mm thick specimens are much more in line with expectations. In Figs 9, 10 and 11, the data are not as well co-ordinated as those recorded by Gencur *et al.* but they do show da/dN increasing fairly systematically with increasing ΔK. The general trend is approximately in accordance with Equation 1, especially when ΔK is above 2.3 MPa $m^{0.5}$. Such a dramatic change in fracture behaviour with increasing thickness strongly suggests that sporadic fatigue crack propagation in UHMWPE is caused by plane strain loading at the crack tip, applied repeatedly to an imperfectly-consolidated sample.

The standard criterion for plane strain loading at a crack tip in a linear elastic solid is

$$a \geq 2.5\left(\frac{K_{IC}}{\sigma_Y}\right)^2 \tag{2a}$$

and

$$B \geq 2.5\left(\frac{K_{IC}}{\sigma_Y}\right)^2 \tag{2b}$$

and

$$(W - a) \geq 2.5\left(\frac{K_{IC}}{\sigma_Y}\right)^2 \tag{2c}$$

where B: specimen thickness, W: width, σ_Y: yield stress and K_{IC} is the critical value of K_I at crack initiation. For fatigue tests, K_{IC} is taken as the maximum value of K_I in a loading cycle that produces an increment of crack growth. Because ΔK (and therefore K_{IC}) increases continually with increasing crack length during standard fatigue tests, the fraction of a thick, notched specimen that is subjected to plane strain loading gradually shrinks as the test proceeds. At the same time, the strain energy release rate at each step in crack growth (and

2 The powder particles were between 0.4 and 0.8 μm in diameter – see Part 2 in this series.

therefore the crack speed) increases rapidly. Both factors control fatigue crack propagation in ductile polymers in ways that are well understood. The results obtained during the present study show that there are exceptions to these well-established rules.

The predicted effects of specimen thickness B on the crack tip stress field are illustrated schematically in Fig. 12 for a selection of yield stresses. Each of the three curves defines an area in which K_{Imax} is low enough to satisfy Equations (2a–c), so that specimens remain fully in plane strain throughout any loading-unloading cycle that does not cross the relevant curve. However, it is not necessary to restrict the analysis of erratic fatigue behaviour to specimens that remain fully in plane strain throughout each cycle. It is quite possible for cohesive failure to occur at the crack tip in incompletely-bonded samples, even when only 50 % of the tip (for example) is in plane strain.

For thermoplastics, the yield stress is a function of strain rate and temperature, both of which therefore play an important part in determining whether a specimen is fully in plane strain. In fatigue tests at 3 Hz, K_I continually rises from minimum to maximum in one sixth of a second, so that strain rates are much higher than in standard tensile tests. Cyclic loading also generates heat and raises temperatures at the crack tip. Both factors have to be taken into account when discussing the effects of plane strain loading on material close to the crack tip in an imperfectly-consolidated fatigue specimen. Those factors probably contribute to the irregularities shown in Fig. 7, which extend to testing at $\Delta K = 3.4$ MPa m$^{0.5}$.

Three curves show the effects of varying yield stress on critical conditions. The double arrow marks the limits along the stress intensity axis within which specimens oscillate during a test at $\Delta K = 1.0$ MPa m$^{0.5}$ with $R = 0.1$. Its positioning at $B = 5$ mm is arbitrary; the same limits $K_{min} = 0.1$ MPa m$^{0.5}$ and $K_{max} = 1.1$ MPa m$^{0.5}$ apply at all thickness. The diagram shows that a specimen with $\sigma_y = 20$ MPa and $\Delta K = 1.0$ MPa m$^{0.5}$ is fully in plane strain when $B = 10$ mm, but not when $B = 4$ mm. That would explain why it was so difficult to produce conventional patterns of crack propagation in standard fatigue tests on the 10 mm thick UHMWPE specimens supplied by the polymer producer. Unless ΔK is kept at a relatively high level from the beginning, crazes will form around the crack tip under plane strain conditions during the early stages of a fatigue test and continue to affect crack propagation in an unpredictable manner throughout the test. In the present study, stable crack propagation was initiated and maintained only in one single test, at constant $\Delta K = 2.25$ MPa m$^{0.5}$ – see Fig. 5. Another factor affecting that specimen is the relatively high crack growth rate of about 2.5 μm per cycle, which at a frequency of 3 Hz could take the crack tip forward far enough in each cycle to prevent the formation of a persistent damage zone. A fresh plastic zone would be created ahead of the fresh tip during every cycle, before any new crazes could form.

The stresses close to a sharp crack tip in a linear elastic solid are given by the Westergaard equations, which can be written:

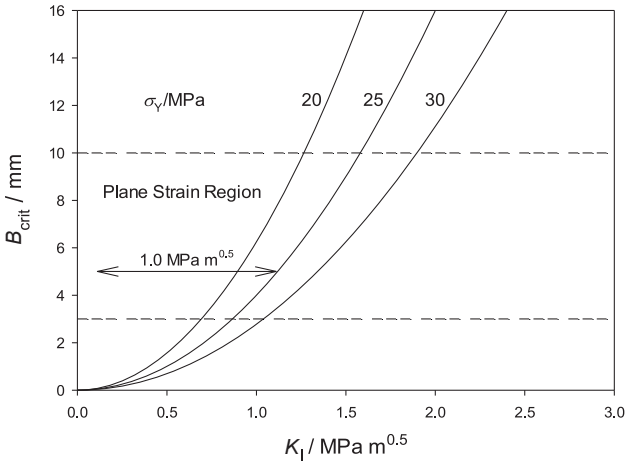

Fig. 12: Relationship between the imposed stress intensity factor, K_I and B_{crit}, the critical specimen thickness required to produce full plane strain conditions at a crack tip, in standard fatigue tests at $R = K_{min}/K_{max} = 0.1$.

$$\sigma_1 = \frac{K_I f_1(r,\theta)}{(2\pi r)^{0.5}} \tag{3}$$

$$\sigma_2 = \frac{K_I f_2(r,\theta)}{(2\pi r)^{0.5}} \tag{4}$$

$$\sigma_3 = \nu(\sigma_1 + \sigma_2) \quad \text{in plane strain} \tag{5a}$$

$$\sigma_3 = 0 \quad \text{in plane stress} \tag{5b}$$

where K_I is the opening-mode crack tip stress intensity, r and θ are polar co-ordinates which have their origin at the crack tip, σ_1 is the local crack-opening tensile stress near the crack tip, σ_2 is the local tensile stress parallel to the direction of crack propagation, σ_3 is the local through-thickness tensile stress, and ν is Poisson's ratio. On the crack plane, the geometric functions f_1 and f_2 simplify as follows

$$f_1(r,\theta) = f_2(r,\theta) = 1$$

and

$$\sigma_3 = 2\nu\sigma_1 \quad \text{in plane strain}$$

As Poisson's ratio for linear polyethylene is 0.46, the ratio of principal stresses on the crack plane is 1:1:0.92 and the mean stress near a sharp notch tip in a thick compact tension is 2.92 $\sigma_1/3$, which is approximately equal to 0.97 σ_1. In other words, under ideal constraint conditions, the material at the crack tip is close to pure triaxial tension in a thick, sharply-notched specimen. Although crack tips in polyethylene are never perfectly sharp in practice, and the polymer is also susceptible to cavitation which could reduce constraints, it is clear that constraints on yielding are usually very high in fatigue tests on UHMWPE.

Ultra-high molecular weight polyethylene is not the only polymer that displays sporadic fatigue crack propagation. Highly erratic behaviour was also observed in an earlier study at the University of Bayreuth, where the same automatic data recording system was used to monitor crack growth in two batches of polypropylene with different crystal structures [7]. The first batch contained a commercial nucleating agent, which produced 'normal' mouldings with 100 % α-PP crystals. The second was blended with an experimental nucleating agent, which formed mouldings with 80 % β-PP phase. Fig. 13 compares fatigue test data obtained from the two sets of mouldings. The specimen with 100 % α-crystallinity gave well co-ordinated results, producing an almost exemplary Paris plot, while the data from the specimen with 80 % β-crystallinity are widely scattered and shifted to higher ΔK levels, indicating a substantially higher resistance to crack propagation. In passing, it should be noted that the results from the α-PP sample show how well Bayreuth University's data-recording system works when applied to well-consolidated specimens.

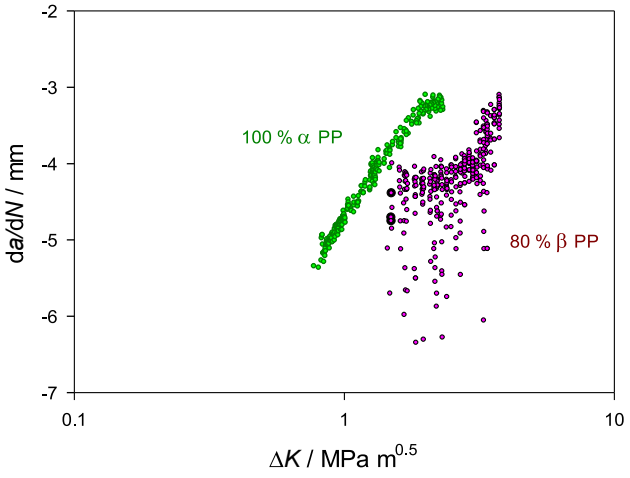

Fig. 13: Fatigue crack data from tests on two polypropylene samples, one containing 100 % of the alpha phase, the other having 80 % beta phase [7].

The crack propagation rates recorded in the present report are based on force-deflection measurements, rather than visual observations, and are calculated on the assumption that every compact tension specimen behaves as a linear elastic solid, except for a very small plastic zone at the crack tip, which remains sharp throughout the test. Fig. 13 demonstrates that this principle works well when the specimens are composed entirely of α-PP, which is well consolidated, but not when they consist largely of β-PP and consolidation is relatively weak. Poorly consolidated samples tend to degrade mechanically around the crack tip when they are subjected to cyclic loading. In both β-PP and weakly-bonded UHMWPE, the degradation process probably involves conversion of type 2 fusion defects, in which a limited amount of entanglement has taken place across the interfaces between powder particles, into type 1 defects, where there are no interfacial entanglements. The Type 1 defects then initiate crazes.

Crazing around a crack tip produces an increase in specimen compliance that does not involve true crack growth. Since the Bayreuth software cannot distinguish between the two mechanisms, it mistakenly attributes the changes in compliance to small increases da in crack length and wrongly reduces the force amplitude at the loading pins in order to keep ΔK constant at a selected level. Thus, Fig. 4 shows the crack tip advancing in roughly equal steps of about 2 μm during the test at $\Delta K = 2.3$ MPa m$^{0.5}$, while it is clear from the data presented in Fig. 3 that the number of cycles between successive steps increased during that test from one to over 1000, as the craze zone at the crack tip expanded and the energy available for crack propagation decreased. This pattern of behaviour indicates that true crack propagation occurred in this test only when the whole compact tension specimen behaved as a defect-free elastic solid (except for a very small yield zone at the crack tip). In other words, at that stage it contained no crazes capable of significantly reducing the energy available for crack growth. Exactly how that state of renewal was achieved is unclear. One possibility is that prolonged cycling at constant crack length weakened the crack-tip craze zone so much that it failed catastrophically, thereby enabling the crack tip to jump forward by 2 μm into a craze-free zone. The whole sequence was then repeated.

Similar principles can be applied to all the other fatigue data from tests on 10 mm thick PE5 specimens, except for those featured in Fig. 5, where da/dN remained constant at about 2 μm per cycle throughout the test. In Fig. 6, the crack growth pattern at $\Delta K = 2.0$ MPa m$^{0.5}$ is similar to that shown in Fig. 3; there is a steady reduction in ΔK, but the test frequency is lower. Raising ΔK to 2.1 MPa m$^{0.5}$ enabled crack propagation to dominate.

The insights gained from this analysis help to explain the extraordinary fatigue behaviour illustrated in Figs. 1 and 2. The results suggest that it was impossible to generate crack growth in 10 mm thick PE06 specimens at $\Delta K < 1.4$ MPa m$^{0.5}$ because cyclic loading at low stress intensity levels initiated distributed crazing from weak grain boundaries, thereby reducing the strain energy release rate at the original crack tip. Because the Bayreuth software attributed all such increases to crack propagation, the software program reduced the applied force amplitude at the loading pins in an attempt to maintain ΔK at the required value. The same problem affected the data recorded by the software throughout almost all of the tests. It was particularly acute in PE06, which has the highest yield stress and therefore remains in plane strain over the largest range of ΔK values – see Figs. 1 and 12 in Part 3 gives $\sigma_Y = 26$ MPa for PE06, but only 20 MPa for PE5 and PE9.

At $\Delta K > 2.5$ MPa m$^{0.5}$, da/dN oscillates sporadically in Fig. 1, in a similar manner to that illustrated in Fig. 6. In both specimens, true crack growth is combined with the growth (and occasional partial failure) of an accompanying craze zone. The increased compliance of the specimen due to extensive crazing is misinterpreted by the software as true crack propagation, but the error is corrected when the crack breaks through that area of the craze zone. The most puzzling data in Figs. 1 and 2 are those in which the recorded value of da/dN remained precisely constant at 46.820 nm per cycle for 45 000 cycles, while ΔK was raised from 1.6 to 2.6 MPa m$^{0.5}$. Obviously, that is not what happened. For some unknown reason, possibly because crack propagation stopped completely, the software locked onto a specific growth rate and added it to the data record repeatedly until the crack tip finally moved forward and new readings were taken. That problem can be resolved only by making changes to the software.

Figures 9–11 show how reducing the thickness of the compact tension specimens from 10 to 4 mm alters the fatigue behaviour of all three grades of UHMWPE. There are still some irregularities, especially in the PE06 specimen at $\Delta K < 2.3$ MPa m$^{0.5}$, but they are not on the same scale as those exhibited by the 10 mm thick

mouldings. While they were probably caused by incomplete consolidation in the mouldings, there is no conclusive evidence to support that interpretation.

Consolidation in UHMWPE depends critically on the formation of entanglements across grain boundaries. The factors controlling this process include:

a. average chain length and chain length distribution
b. levels of entanglement formed in powder particles during polymerization
c. types and concentrations of additives (*e.g.* Vitamin A) in the melt
d. method of conversion from powder to consolidated block
e. times, temperatures and pressures applied during melt processing

Sintering of UHMWPE is a complex process. It begins with densification of the powder, so that the surfaces are brought fully into contact and wetted, both of which can be accomplished below the melting point of the polymer. Then, in a second stage at a higher temperature, chains diffuse across grain boundaries, fresh entanglements are formed, and the material is consolidated. Earlier authors modelled consolidation using classic reptation theory, but Deplancke *et al.* have demonstrated that diffusion and entanglement across grain boundaries can take place much more rapidly than is predicted by reptation-based models by following different kinetics [8, 9]. Working on UHMWPE mouldings made from as-polymerized reactor powder, they carried out tensile tests at 200 °C, which showed the effects of sintering time, t_s, on stress-strain curves to be relatively small, with t_s ranging from 0.25 to 100 h, while sintering temperature had a much stronger effect on mechanical properties. From these observations, Deplancke *et al.* concluded that chain diffusion and entanglement are dominated by 'sideways' motions (normal to the chain axis) of large chain loops, which are able to bond particles together much more rapidly than chain-end reptation. In samples subjected to long sintering times, reptation still plays a part, but a secondary one. In the present context, the speed at which chain loops bond particles together during compression moulding raises questions about their ability to resist gradual pullout during fatigue tests on thick specimens at room temperature.

The main causes of the extraordinary fatigue crack growth behaviour displayed by PE06, PE5 and PE9 are the extreme lengths of their chains, which hinder consolidation, and the thicknesses of the compact tension specimens, which impose constraints on plastic zones at crack tips, but those are not the only significant factors. As noted earlier, Gencur *et al.* [5] observed perfectly conventional fatigue crack propagation in experiments on 10 and 20 mm thick specimens, which were machined from ram-extruded rod made from a commercial grade of UHMWPE. In addition to differences in processing conditions, possible reasons for the strong contrast in fatigue behaviour between the ram-extruded and compression-moulded specimens include their composition and the intervals between melt processing and testing. The compression mouldings prepared for this project contained no additives, but there is no available information about the composition of the commercial grade used by Gencur *et al.* Also, there was a delay of at least 5 years between the moulding and testing of the IUPAC samples, while the delay between ram extrusion and testing by Gencur *et al.* was probably much shorter.

It is important to distinguish between the highly localized damage mechanisms responsible for sporadic fatigue crack propagation in PE06, PE5 and PE9, which appear to be restricted to a very small region close to the crack tip, and the type of cavitation that occurs during plastic deformation and fracture in all grades of polyethylene and is largely responsible for the polymer's high fracture toughness. That more familiar, beneficial mode of cavitation takes place on a larger scale and enables the polymer to draw and strain-harden internally, usually without incurring failure in any of the load-bearing main-chain bonds. Strong, porous notch-tip plastic zones are able to expand, absorbing a large amount of energy. That mechanism of toughening is illustrated in a review by Medel and Furmanski [6], which includes an optical micrograph of a low-density 'cohesive zone' at the tip of a fatigue crack in a side-grooved compact tension specimen – see Fig. 30.5 in the third edition of the UHMWPE Biomaterials Handbook [6]. It is clear that the porous plastic zone contains voids with dimensions in the region of 50 μm, but the detailed structure of the zone is difficult to distinguish because of the long optical path through the cavitated zone.

Fatigue testing of mouldings containing various amounts of different additives would be one obvious avenue to explore in any future project. A possible factor affecting the sporadic crack propagation observed in this project is that the omission of antioxidants and other stabilizers resulted in some chemical degradation, either at the melt processing stage or during subsequent storage. As the fatigue tests described in this article were carried out long after the mouldings were manufactured, the effects of long-term degradation cannot be completely discounted.

In orthopaedic applications, the most critical form of damage in UHMWPE is not fatigue crack growth, but wear. The problem is most acute in knee joint replacements, which not only suffer losses of material from heavily loaded bearing surfaces, but also generate wear debris particles, which have diameters mainly in the range 0.1 to 10 μm – see Part 3 in this series [10–13]. The body's immunological response to these particles is complex; it includes both inflammation and bone loss (osteolysis), which in the most severe cases leads to loosening of the implant and the need for replacement surgery. The precise mechanisms responsible for the formation of wear debris are unclear, but it is reasonable to conclude that cohesive failure of weak bonds between particles about 1 μm in diameter plays an important part in the process. Thus, the observations of sporadic fatigue crack growth in PE06, PE5 and PE9 might throw some light on the formation of wear debris and fatigue testing could perhaps provide an effective method for investigating the factors controlling wear resistance in UHMWPE.

The principal method used to increase wear resistance in orthopaedic grades of UHMWPE is radiation-induced crosslinking, followed by post-irradiation thermal treatment. This treatment reduces wear rates, but substantially reduces resistance to fatigue crack growth. There is little commercial incentive to address this problem, because fatigue fracture accounts for only a small proportion of failures in polymer-based implants, but it is nevertheless a significant problem.

Another important conclusion to be drawn from Figs. 1, 3, 6 and 13 is that the main effect of sporadic crack growth is to increase, rather than decrease, resistance to crack propagation. In other words, the mechanism responsible for the exceptional fatigue behaviour displayed by PE06, PE5 and PE9 is in some ways similar to multiple crazing, which is a cohesive failure mechanism that enables rubber-toughened thermoplastics, such as acrylonitrile-butadiene-styrene copolymer (ABS) and high-impact polystyrene, to absorb large amounts of energy in impact tests.

4 Conclusions

Fatigue tests were carried out on 10 mm thick compact tension specimens cut from compression mouldings supplied by a leading manufacturer of UHMWPE. The results obtained during these tests were extremely unusual and clearly indicate that the mouldings were not fully consolidated. Alternative methods, including fatigue testing on thin CT specimens, standard tensile tests, and small punch tests, were unable to distinguish between imperfect and well-consolidated samples. Thus, the manufacturers who supplied compression mouldings for this project were unaware of a potential problem until they received the results presented in this report. In light of these findings, there is a case for introducing a new quality-assurance standard for melt-processed UHMWPE, based on fatigue testing.

5 Overview of project

This project was initiated by IUPAC Sub-Committee 4.2.1 because of concerns about quality control and quality assurance procedures for orthopaedic grades of UHMWPE. It received strong support, not only from members of the main sub-committee, which is currently based in Europe, but also (for the first time) from members from the East Asian Group. That in itself was a success. The broad scope of the project also enabled specialists with diverse interests, ranging from melt rheology to mechanical properties, to make meaningful contributions to the program of work.

The role of entanglements was a central issue at all stages of the project. Some are formed in the polymerization reactor, because catalytic sites are closely spaced in order to maximize rates of reaction. It is therefore almost impossible to prepare gel-free solutions, which are needed for size-exclusion chromatography, and also quite difficult to produce satisfactory solutions for intrinsic viscosity testing, where gel formation can affect measured viscosities. There are disagreements between experts on whether shaking or stirring is the best way to prepare solutions. The entanglements formed during melt processing make it impossible to make meaningful IV measurements.

If $\overline{M}_W$ is high enough, as it is in PE5 and PE9, these problems can be circumvented by carrying out creep tests at 150 °C, just above the melting point, following ASTM Standard D4020 [13]. The values of $\overline{M}_W$ obtained in this way during the present project were rather lower than those obtained from intrinsic viscosity measurements and raise questions about the reason for the difference. One obvious factor is that the equations recommended by international standards are based on the assumption that the test samples are homogeneous, with an entanglement density that has reached its optimum level, so that the results are not affected by weakly bonded grain boundaries. That assumption is perfectly valid for cast poly(methyl methacrylate) (PMMA), but not necessarily for compression moulded UHMWPE. In the mouldings provided for this project, grain boundaries were clearly visible, and the assumption of homogeneity was invalid. That might explain why the high-temperature creep data obtained by Liu gave $\overline{M}_W$ as 3.8 and 5.6 MDa for PE5 and PE9, respectively (see Part 1), whereas intrinsic viscosity tests carried out by the manufacturer gave 5.7 and 8.5 MDa, respectively. This explanation could be tested by making fresh 10 mm thick plaques under a range of processing conditions and using creep measurements at 150 °C to determine whether calculated values of M_w are dependent on those conditions.

The effects of chain entanglements on the properties of mouldings are also seen clearly in Part 2 of this series. As reactor powders, all three grades of UHMWPE had similarly high levels of crystallinity, at about 70 %, but these fell after compression moulding to 60 %, in the case of PE06, and to about 45 % in PE5 and PE9. Because of the higher levels of entanglement in PE5 and PE9, rates of reptation during cooling were too low to enable χ_c to reach 70 %.

The mechanical test data presented in Part 3 show large differences in stress-strain behaviour between PE06 and PE5, but much smaller differences between PE5 and PE9. At small strains deformation is essentially elastic, and dominated by crystallinity, which is substantially higher in PE06 than in PE5 and PE9. These differences are due to longer relaxation times during cooling in the mould in the two true UHMWPE grades. Beyond the yield point the effects of entanglement density became increasingly dominant, so that rates of strain hardening were higher in PE5 and PE9 than in PE06. However, the differences between PE5 and PE9 were smaller than predicted, and in some tests were negligible, because the predictions were based on the assumption that the mouldings were fully consolidated and that entanglement levels could therefore be calculated from the measured molecular weights. On the basis of this evidence it is concluded that neither PE5 nor PE9 were fully consolidated during compression moulding.

The most striking experimental data generated during the project were those obtained from fatigue tests on thick compact tension specimens – see Sections 1–4 of this report. They provide answers to the main questions addressed by this project: (a) is there a convenient test that can distinguish between an incompletely consolidated sample of UHMWPE and a completely consolidated one? and (b) Is it possible to make a quantitative assessment of the extent to which the sample comes close to complete consolidation? This study has shown that fatigue testing of thick specimens can provide information about significant deviations from complete consolidation and can open the path to further investigation in this area. As the UHMWPE manufacturer that supplied mouldings for this project does not wish to disclose details about its processing conditions, the next step towards understanding the factors controlling consolidation of UHMWPE powder is obviously to prepare more thick plaques over a range of well-documented processing conditions and use fatigue testing as a QA procedure.

6 Membership of sponsoring bodies

Membership of the Subcommittee on Structure and Properties of Commercial Polymers during the preparation of these Reports was:
Chair: Yongfen Men (China); **Secretary:** Yujing Tang (China); **Members:** Volker Altstädt (Germany); Lijia Am (China); Oliver Arnolds (USA); Dietmar W. Auhl (Netherlands); Paul Buckley (UK); Clive B. Bucknall (UK); Peng Chen (China); lldoo Chung (S. Korea); Dirk J. Dijkstra (Germany); Andrzej Galeski (Poland); Christoph Gögelein (Germany); Chang-Sik Ha (S. Korea); Mijeong Han (S. Korea); Ulrich Handge (Germany); Jiasong He (China); Sven Henning (Germany); Jun-ichi Horinaka (Japan); Wenbing Hu (China); Dae Woo Ihm (S. Korea); Tadashi Inoue (Japan); Takaharu Isaki (Japan); Akihiro Izuka (Japan); Xiangling Ji (China); Michail Kalloudis (UK); Dukjoon Kim (S. Korea); Jin Kon Kim (S. Korea); Sung Chul Kim (S. Korea); Seong Hun Kim (S. Korea); D. Su. Lee (S. Korea); Won-Ki Lee (S. Korea); Jae Heung Lee (S. Korea); Soonho Lim (S. Korea); Chengyang Liu (China); Shu-ichi Maeda (Japan); Mario Malinconico (Italy); Goerg Michler (Germany); Koh-Hei Nitta (Japan); Ewa Piorkowska-Galeska (Poland); Jinliang Qiao (China); Artur Rozanski (Poland); Dong Gi Seong (S. Korea); Tongfei Shi (China); Hongwei Shi (China); Sampat Singh Bhatti (Germany); Miroslav Slouf (Czech Republic); Zhaohui Su (China); Toshikazu Takigawa (Japan); Katsuhisa Tokumitsu (Japan); Kenji Urayama (Japan); Tatana Vackova (Czech Republic); Silvie Vervoort (Netherlands); Iakovos Vittorias (Germany); Yanwei Wang (Kazakhstan); Jun Jie Wu (UK); Donghua Xu (China); Masayuki Yamaguchi (Japan); Myung Han Yoon (S. Korea); Wentao Zhai (China); Wim Zoetelief (Netherlands)
Membership of the IUPAC Polymer Division Committee for the period 2020–2021 is as follows:
President: C. K. Luscombe (USA); **Past President:** G. T. Russell (New Zealand); **Vice President:** I. Lacík (Slovakia); **Secretary:** P. D. Topham (UK); **Titular Members:** M. C. H. Chan (Malaysia); C. Fellows (Australia); R. C. Hiorns (France); R. Hutchinson (Canada); D. S. Lee (Korea); John B. Matson (USA); **Associate Members:** S. Beuermann (Germany); G. Moad (Australia); Marloes Peeters (UK); C. dos Santos (Brazil); P. Théato (Germany); M. G. Walter (USA); **National Representatives:** Ana Aguiar-Ricardo (Portugal); Jiasong He (China); C.-S. Hsu (Taiwan); Melina T. Kalagasidis Krušić (Serbia); P. Mallon (South Africa); O. Philippova (Russia); Guido Raos (Italy); M. Sawamoto (Japan); A. Sturcova (Czech Republic); Jan van Hest (Netherlands).

Acknowledgements: The authors thank the polymer manufacturer for supplying compression mouldings of various thicknesses for this project, and the students and research staff who contributed to it: Richard Dusin (Lanxess) D. Di Francesco (Durham), Przemyslaw Sowinski (Lodz), Qian Qiang Wang (Durham), Kinga Zapala (Lodz), Alexander Brückner and Rico Zeiler (Bayreuth).
Research funding: Project 2010-019-1-400 was supported by a grant from IUPAC.

References

[1] M. H. Kothmann. *Polymer* **60**, 157 (2015).
[2] U. A. Handge. *J. Appl. Polym. Sci.* **124**, 740 (2012).
[3] Z. P. Zeng, M. Buggy, J. Griffin, E. G. Little. *J. Mater. Sci.: Mater. Med.* **3**, 255 (1992).
[4] L. A. Pruitt. *Biomaterials* **26**, 905 (2005).
[5] S. J. Gencur, C. M. Rimnac, S. M. Kurtz. *Biomaterials* **27**, 1550 (2006).
[6] S. M. Kurtz. *UHMWPE Biomaterials Handbook*, Elsevier, Amsterdam, 3rd ed. (2015).
[7] M. Kersch, L. Pischke, H.-W. Schmidt, V. Altstädt. *Polymer* **55**, 3227 (2014).
[8] T. Deplancke, O. Lame, F. Rousset, I. Agulli, G. Vigler. *Macromolecules* **47**, 197 (2014).
[9] T. Deplancke, O. Lame, F. Rousset, R. Seguela, G. Vigler. *Macromolecules* **48**, 5328 (2015).
[10] K. G. Plumlee, C. H Schwarz. *Wear*, Part A, **426**,171 (2019).
[11] A. Sirimamilla, C. M. Rimnac. *J. Mech. Behavior Biomed. Mater.* **91**, 366 (2019).
[12] K. M. Varadarajan, E. Oral, O. K. Muratoglu, A. A. Freiberg *Tech. Orthop.* **33**, 17 (2018).
[13] ASTM Standard D4020-18. *Standard Specification for Ultra-High-Molecular-Weight Polyethylene Molding and Extrusion Materials*. ASTM International, West Conshohocken, PA (2018), www.astm.org.